Technical Paper
Journal of Aerospace System Engineering
Vol.15, No.4, pp.21-29 (2021)
EISSN 2508-7150
http://dx.doi.org/10.20910/JASE.2021.15.4.21

Comparative Analysis of the PWM of an Inverter for an Electric Aircraft Thrust Motor

Bon-soo Koo[1,†], Seong-hyeon Jo[2], and In-ho Choi[1]
[1]Korea Aerospace Research Institute
[2]Pusan National University

Abstract

As global environmental regulations have been strengthened, the eco-friendly market has grown rapidly. In the field of aircraft, research on electric vertical take-off and landing aircraft that can enter city centers and perform personal air transportation using electric propulsion is ongoing. For aircraft using electric propulsion methods to operate reliably, electric power thrust systems are a key factor. Electric aircraft require a high power density for propulsion systems with strict limits on volume and weight. The efficient control of inverter systems is essential for achieving high power density. Therefore, in this paper, the characteristics of inverters and motors were analyzed through simulations based on the space vector pulse width modulation (PWM) and discontinuous PWM methods for controlling inverter systems.

Key Words : Electric Propulsion, Electric Aircraft, Inverter, PWM, Aircraft Electric Motor

1. Introduction

According to the global trend of increasingly tightened environmental regulations, the eco-friendly market has exhibited remarkable growth. In the aircraft sector, research is being conducted on electric vertical take-off and landing (eVTOL) aircraft that facilitate entry into city centers and personal air vehicle transportation based on next-generation transportation vehicles with electronic propulsion [1].

For the reliable operation of electric aircraft, electric power thrust systems play a pivotal role. Electric aircraft require propulsion systems with high power density as a result of strict limits on total volume and weight. To satisfy the high power density requirements of electric propulsion systems, high-efficiency inverter systems with good reliability and low vibration are required [2].

In this study, the pulse width modulation (PWM) method was analyzed as a core technology for inverters for controlling electric motors, and inverter and motor characteristics were analyzed according to the modulation methods of space vector PWM (SVPWM) and discontinuous PWM (60DPWM) through simulations. For our simulations, the PSIM tool provided by Powersim was adopted. PSIM is an electronic circuit simulation software designed for the simulation of electric devices and motor drives [3]. The SVPWM and 60DPWM methods were considered for the simulation of phase current total harmonic distortion (THD), inverter switching loss, and motor torque ripple. By analyzing the simulation results, a method for operating inverters with consideration for switching loss and the allowable range of noise levels was developed.

Received: Oct. 12, 2020 Revised: Feb. 17, 2021 Accepted: Mar. 05, 2021
† Corresponding Author
Tel: +82-42-860-2894, E-mail: bonsoo@kari.re.kr

2. Motor & Inverter

A three-phase permanent magnet synchronous motor (PMSM) was considered in this study as a high-power/high-efficiency lightweight motor that has been widely used in electric aircraft in recent years. To control the PMSM motor, a current controller setup was designed to utilize feedback from a position sensor attached to the motor and a current sensor, as shown in Fig. 1 [1].

The voltage commands from the current controller are executed by a power converter composed of power semiconductors such as insulated gate bipolar transistors (IGBTs) or metal-oxide semiconductor field effect transistors and applied to the motor. Generally, a three-phase inverter module is used. Therefore, if the voltage commands are executed through PWM, as a result of the inductance of the motor coil, the current waveform is generated in the form of a sine wave with ripple components

[4]. In this case, because the switching frequency for the power semiconductors and test conditions vary depending on the modulation method, the current ripple and loss are affected and the THD, motor torque ripple, and inverter efficiency are modified according to the ripple component of the phase current [5].

Four PMSMs were selected as a candidate group for the final design of an aircraft motor. When selecting the candidate group, motors with a maximum power between 90 kW and 100 kW were selected. The selected candidate motors were the AC35 Dual from HPEVS with a maximum power of 96 kW, YASA 400 from YASA with a maximum power of 90 kW, Zero 75-7 from Zero Motorcycles with a maximum power of 100 kW, and EMRAX228 from EMRAX with maximum power of 109 kW. Based on the nature of electric propulsion aircraft, strict limits on volume and weight are imposed. Therefore, the power density of the electric motors was prioritized among the criteria for selecting an aircraft motor [3]. We calculated the power densities of the candidate motors and determined that the AC35 has a power density of 1.4 kW/kg, EMRAX228 has a power density of 8.13 kW/kg, YASA 400 has a power density of 3.75 kW/kg, and Zero 75-7 has a power density of 3.15 kW/kg. When comparing the motors in the candidate group based on power density, the EMRAX228, which has the highest power density, was selected as an appropriate aircraft motor. However, for the actual motor analyzed in this study, the EMRAX208 was selected. This motor is one level lower than the EMRAX228 motor and was more suitable for the motor generator test environment. The maximum torque of the EMRAX208 water-cooled motor is 75 kW, its weight is 9.1 kg, and its power density is 7.97 kW/kg [3].

The inverter for the control of a PMSM consists of six switches and switching loss occurs during the operation of on/off switching. The inverter receives DC power as an input and outputs three-phase AC power for motor control.

When the inverter is operated with a high frequency switching, it is possible to achieve improvement in the waveforms through harmonic reduction and the reduction of the size and weight of the filters and devices, but switching loss increases with an increase in the switching frequency. This loss leads to problems such as heat generation, reduced reliability, and shortened service life. Therefore, reducing heat dissipation and loss is a crucial factor determining the service life and price of switching devices, and the volumes of coolers [6].

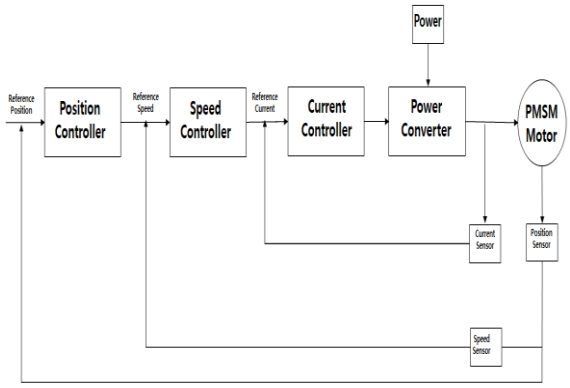

Fig. 1 Inverter block diagram

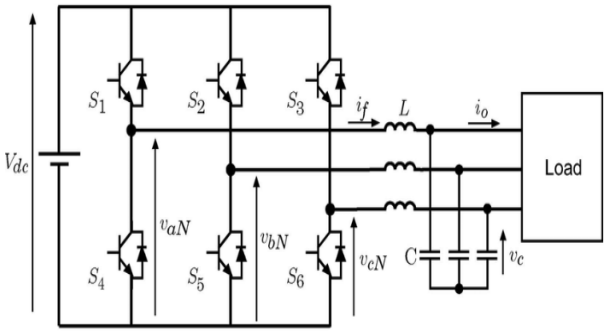

Fig. 2 Three-phase inverter

2.1 Electrical and Mechanical Properties of the EMRAX208

The EMRAX208 motor is an axial PMSM and has a structure without a yoke, so the volume and core loss can be reduced. The stator and rotor are designed with 20 poles and the motor has sinusoidal back electromotive force (EMF) waveforms. The overall structure is presented in Fig. 3. Regarding the electrical properties of the EMRAX208, the motor has a DC link voltage of 470 Vdc, internal phase resistance of 0.014 Ω, and internal inductance on the d-axis of 125 uH and q-axis of 130 uH, as well as some salient pole characteristics. The torque constant is 0.8 Nm/1Aph rms, back EMF constant is 68.4 Vpk/Arms, and axial magnetic flux is 0.0393 Vs. Regarding the mechanical properties, the moment of inertia is 0.023 kgm^2 and the maximum output power is 75 Kw. The rated current is 100 A and the rated torque is 65 Nm for the water-cooled type [7].

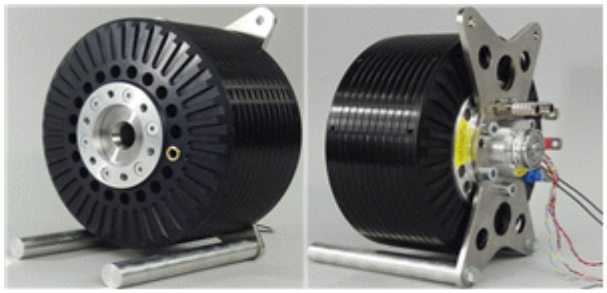

Fig. 3 EMRAX208 motor

2.2 SEMIKRON SKiip 26GB12T4V1 Inverter

The inverter modeled in our simulations was a SKiip 26GB12T4V1 IGBT from SEMIKRON. Inverter modeling was performed based on the characteristic parameters of the inverter from its data sheets, as shown in Figs. 4 and 5. Regarding the electrical characteristics of the inverter, the maximum values are $V_{ce}=1200\ V, I_c=290A$, temperature range is $T_j=-40\sim 175^\circ C$, and switching turn-on/off energy is $E_{on}=13.6\ mJ, E_{off}=22.1\ mJ$ under a junction temperature of 150 °C. Other key features include a Trench 4 IGBT, robust and freewheeling diodes using CAL technology, highly reliable spring contacts for electrical connections, and negative-temperature-coefficient temperature sensor [8].

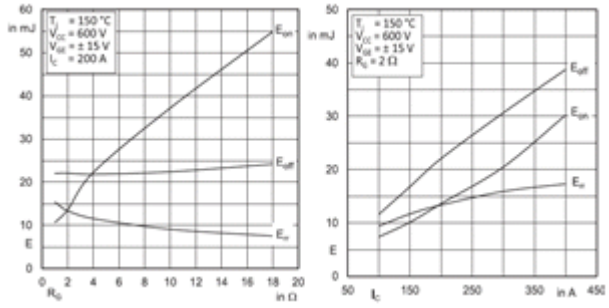

Fig. 4 Turn-on/off energy= f(RG), turn-on/off energy= f(IC)

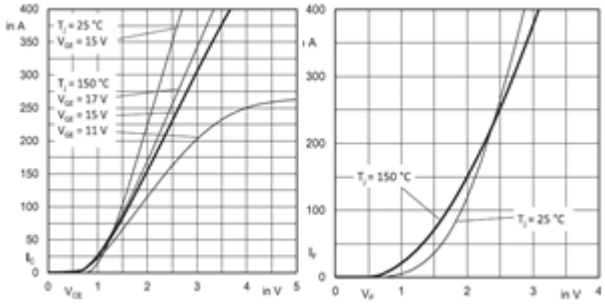

Fig. 5 Output characteristic: inclusive RCC'+ EE' CAL, diode forward characteristic: inclusive RCC'+ EE

3. PWM Inverter

To control the rotation speed of a motor and obtain fast responses through the rapid supply of the reference current generated by the vector control algorithm to the stator of the motor, an inverter with a high switching frequency should be adopted. To control the sine wave current using an inverter in this manner, a PWM method with high-speed switching devices should be employed [9]. When an inverter with the PWM method is used, it is possible to perform linear control of the magnitude of the fundamental wave of the output voltage, control harmonic components, and control the frequency of the fundamental wave of the output voltage.

The main role of the PWM technique is to generate gating pulses for the on/off switching of the virtual switch such that the inverter can generate a fundamental wave voltage of the same magnitude and frequency as the command voltage. When driving a motor with an inverter, the final motor torque is determined by the current, so evaluation of the harmonic content in the current is considered to be more important than the output voltage.

With the application of the PWM method, the loss and stress of the switching device increase. Therefore, it is necessary to evaluate not only direct switching loss, but also the harmonic loss of the motor caused by the switching voltage.

The PWM method includes a continuous modulation method and discontinuous modulation method. The representative continuous modulation method is min-max PWM, which produces the same effect as SVPWM with simple operations, and the representative discontinuous modulation method is DPWM.

3.1 Space Vector PWM

SVPWM is one of the PWM methods that represents a high three-phase voltage command as a single space vector in a complex vector space and determines the switching time with reference to a single position. Three-phase SVPWM considers all six switches of the three phases and outputs are produced according to hourly calculation results accounting for the switching state of each pole. The SVPWM method is superior to other PWM methods in terms of its voltage utilization ratio and the low harmonic content of the output current, as well as the linearity of control. This method is mainly used in three-phase inverters and converters [6]. Fig. 6 presents the simulation results for the THD of the three-phase current in the input terminal and polar voltage command waveforms when the SVPWM method is applied.

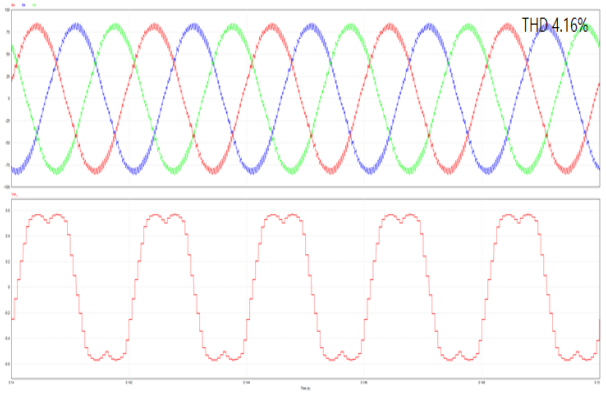

Fig. 6 SVPWM phase current and polar voltage command waveforms

3.2 DPWM

SVPWM is a continuous voltage modulation method in which all elements of the three-level inverter are in the switching state during one cycle. However, to reduce the number of switching

operations, the DPWM technique has been proposed, where only two out of the three phases are in a switching state [6].

DPWM has a feature where the number of switching operations is reduced compared to SVPWM, leading to reduced loss caused by switching. The switching loss and harmonic characteristics vary depending on where the non-switching leg is placed. In a three-phase system, the discontinuous modulation leg in the non-switching state during one cycle of command voltage can be set up to 120°. Depending on the angle, this method is referred to as 30DPWM, 60DPWM, 60(+30°)DPWM, 60(−30°)DPWM and 120DPWM.

Regarding the major characteristics of each modulation method, the 30DPWM method has the best harmonic reduction performance, but provides little contribution in terms of reducing switching loss. The 120DPWM method has the best switching loss reduction performance, but generates significant harmonic components. In comparison, the 60DPWM method has the advantage of reducing switching loss compared to the continuous modulation method and yields reduced harmonic components compared to the 120DPWM method. Therefore, in this paper, the 60DPWM is considered for analysis.

The 60DPWM method reduces the switching frequency by leaving the state on or off without switching operations during the 60° leg of the largest phase voltage over one cycle of phase voltage. Therefore, switching is reduced by one-third in one cycle, meaning the overall switching frequency can be reduced by one-third, indicating a reduction in switching frequency to approximately 67% compared to the continuous modulation method. To minimize the actual switching loss, it is desirable to determine the leg of non-switching operation based on the magnitude of the phase current, rather than the phase voltage. Fig. 8 presents the waveforms for offset voltage and polar voltage commands with different voltage modulation indexes. Fig. 9 presents the waveforms of the three-phase current and polar voltage command.

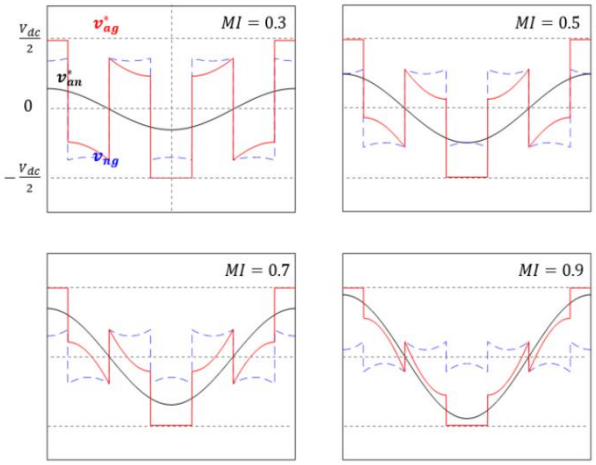

Fig. 7 60DPWM offset voltage and polar voltage commands

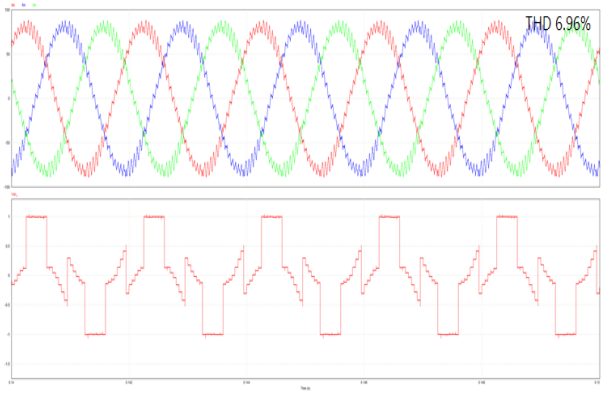

Fig. 8 60DPWM phase current and polar voltage command waveforms

4. Performance analysis

For the performance analysis of a PWM inverter, the phase current THD, switching loss of the inverter, and motor torque ripple were comparatively analyzed according to the different modulation methods of SVPWM and 60DPWM.

4.1 Phase current THD with respect to the PWM inverter

The THD of a signal is a measurement of the harmonic distortion in that signal and is defined as the ratio of the sum of the powers of all harmonic components to the power of the fundamental frequency. The THD is an important factor for describing the quality of a power system. The harmonic components of the phase current affect the dq-axis current. Equations 1 to 4 are formulas for converting the phase current into dq-axis current. The process for the synchronous coordinate system conversion of the harmonic current is defined as follows. First, conversion into the synchronous coordinate system for the nth harmonic component is performed, dq-axis components are calculated according to the remainder (i.e., 0, 1, 2) after dividing the nth harmonic component by three, and the harmonic components are presented as AC components in the synchronous coordinate system, rather than DC components.

Because low THD in a power system leads to reduced peak current, heat dissipation, and loss in motors, THD also serves as an important parameter for aircraft [11].

$$\begin{aligned} i_{as-n} &= -I_{mn}\sin n^*\omega_e t \\ i_{bs-n} &= -I_{mn}\sin n^*(\omega_e t - 120^\circ) \\ i_{cs-n} &= -I_{mn}\sin n^*(\omega_e t + 120^\circ) \end{aligned} \quad (1)$$

$$\begin{aligned} i^s_{dsn} &= -I_{mn}\sin(n^*\omega_e t) \rightarrow i^r_{dsn} = -I_{mn}\sin((n-1)^*\omega_e t) \\ i^s_{qsn} &= I_{mn}\cos(n^*\omega_e t) \rightarrow i^r_{qsn} = I_{mn}\cos((n-1)^*\omega_e t) \end{aligned} \quad (2)$$

$$\begin{aligned} i^s_{dsn} &= -I_{mn}\sin(n^*\omega_e t) \rightarrow i^r_{dsn} = -I_{mn}\sin((n+1)^*\omega_e t) \\ i^s_{qsn} &= I_{mn}\cos(n^*\omega_e t) \rightarrow i^r_{qsn} = I_{mn}\cos((n+1)^*\omega_e t) \end{aligned} \quad (3)$$

$$\begin{aligned} i^s_{dsn} = 0 \rightarrow \quad i^r_{dsn} = 0 \\ i^s_{qsn} = 0 \rightarrow \quad i^r_{qsn} = 0 \end{aligned} \tag{4}$$

4.2 Switching loss with respect to the PWM inverter

In power electronic devices, switching loss has a significant impact on total system loss and is one of the key parameters for analyzing system efficiency. Reducing the switching loss in a system increases the system efficiency at the point of load. Switching loss refers to the loss that occurs when a switch is turned on or off. As shown in Eq. 5, the switching losses of IGBTs and diodes can be expressed as the product of the switching energy and switching frequency [10].

$$\begin{aligned} P_{sw\,Q_{on}} &= E_{on} * f_{sw} * V_{cc} / V_{ccdatsheet} \\ P_{sw\,Q_{off}} &= E_{off} * f_{sw} * V_{cc} / V_{ccdatsheet} \end{aligned} \tag{5}$$

4.3 Torque ripple with respect to the PWM inverter

The torque ripple components of a PMSM mainly affect the accuracy of the motor position and velocity control drive. Additionally, unwanted mechanical vibrations and noise in the motor are generated and ripples are generated in the velocity response of the motor at low speeds, while noise and vibration are generated at high speeds. Therefore, the torque ripple should be controlled to be minimized in areas that are heavily affected by vibration and noise, such as aircraft [10].

The output torque of the motor is expressed in terms of the dq-axis current function and the motor torque ripple is proportional to the dq-axis current of the motor. The torque ripple components are included in the torque and the torque values can be calculated as shown in Eqs. 6 and 7.

$$\begin{aligned} v_{as} &= Ri_{as} + L\frac{di_{as}}{dt} + e_a \\ v_{bs} &= Ri_{bs} + L\frac{di_{bs}}{dt} + e_b \\ v_{cs} &= Ri_{cs} + L\frac{di_{cs}}{dt} + e_c \\ &\Downarrow \\ V^s_{ds} &= Ri^s_{ds} + L\frac{di^s_{ds}}{dt} + e^s_{ds} \\ V^s_{qs} &= Ri^s_{qs} + L\frac{di^s_{qs}}{dt} + e^s_{qs} \\ &\Downarrow \\ V^r_{ds} &= Ri^r_{ds} + L\frac{di^r_{ds}}{dt} - w_r L_{qs} i^r_{qs} \\ V^r_{qs} &= Ri^r_{qs} + L\frac{di^r_{qs}}{dt} + w_r L_{ds} i^r_{ds} + w_r \Phi_f \end{aligned} \tag{6}$$

$$\begin{aligned} P &= \frac{3}{2}(v^r_{ds} i^r_{ds} + v^r_{qs} i^r_{qs}) \\ &\Downarrow \\ &= \frac{3}{2}(R_s(i^r_{ds} + i^r_{ds}) + i^r_{ds}\frac{d\lambda^r_{ds}}{dt} + i^r_{qs}\frac{d\lambda^r_{qs}}{dt} + \\ &\quad w_r \Phi_f i^r_{qs} + w_r (L_d - L_q) i^r_{ds} i^r_{qs}) \leftarrow Pout \end{aligned}$$

$$\begin{aligned} T_e &= \frac{Pout}{w_r} \\ T_e &= \frac{3P}{4}(w_r \Phi_f i^r_{qs} + w_r (L_d - L_q) i^r_{ds} i^r_{qs}) \\ &= \frac{3P}{4}(\Phi_f i^r_{qs} + (L_d - L_q) i^r_{ds} i^r_{qs}) \end{aligned}$$

$$\Phi_f = \frac{V_{pk} * 60}{\sqrt{3} * \pi * P * 1000} \tag{7}$$

4.4 Simulation

To evaluable performance according to the different modulation methods of SVPWM and 60DPWM, the current THD in the a-phase stator winding of the target motor, switching loss of the inverter, and torque ripple of the motor were measured.

Simulations were conducted by modeling the EMRAX208 motor with a high specific power and the Semikron SKiip 26GB12T4V1 inverter using the PSIM tool in Powersim. Regarding the simulation conditions, the switching frequency was increased in steps of 10 kHz in the range of 10–50 kHz and the rotational speed of the motor was increased in steps of 1000 rpm in the range of 1000–5000 rpm. The load was fixed at 65 Nm, which is the rated load condition for the EMRAX208 motor, for the entire simulation. The simulation conditions are outlined in Table 1. The test cases are arranged by switching frequency at the top level.

Table 1 Test Conditions

Test Condition	
Vdc	470 [V]
Switching Freq	10~50K [hz]
Reference RPM	1000~5000
Load	68 [Nm]
Dead Time	1u [s]
EMRAX208 Parameter	
Stator Winding Resistance	0.014 [Ω]
d-axis inductance	125u [H]
q-axis inductance	135u [H]
back EMF constant	68.4 [Vpk/krpm]
poles	20
moment of inertia	0.0256 [kg-m^2]

shaft time constant	100 [s]

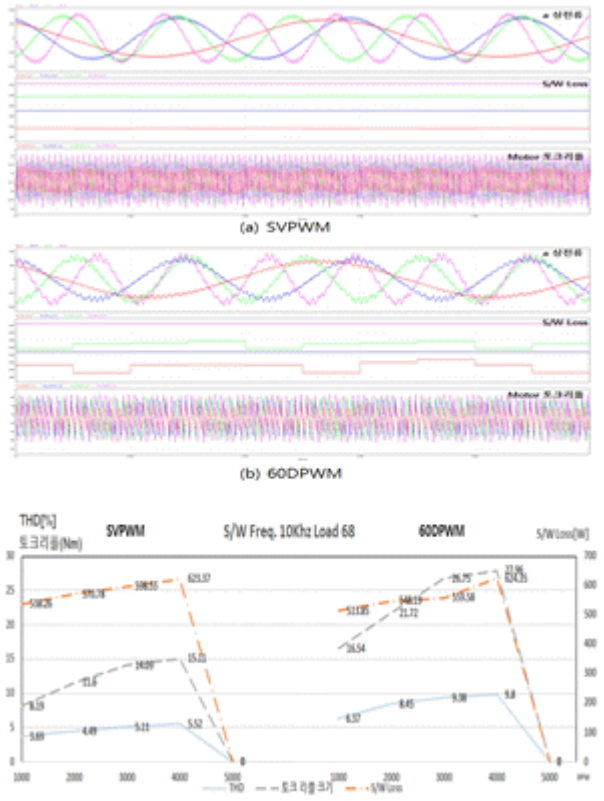

Fig. 9 Switching frequency 10 kHz. Ias THD, Motor torque ripple

Table 2 S/W frequency 10 kHz. Ias THD, S/W Loss, Motor torque ripple

10 kHz	SVPWM			60DPWM		
	THD [%]	S/W Loss [W]	Torque ripple [Nm]	THD [%]	S/W Loss [W]	Torque ripple [Nm]
1000 [RPM]	3.69	538.26	8.19	6.37	513.85	16.54
2000	4.49	570.78	11.6	8.45	548.19	21.72
3000	5.11	598.55	14.09	9.38	559.58	26.75
4000	5.52	623.37	15.11	9.8	624.35	27.96
5000	Divergence					

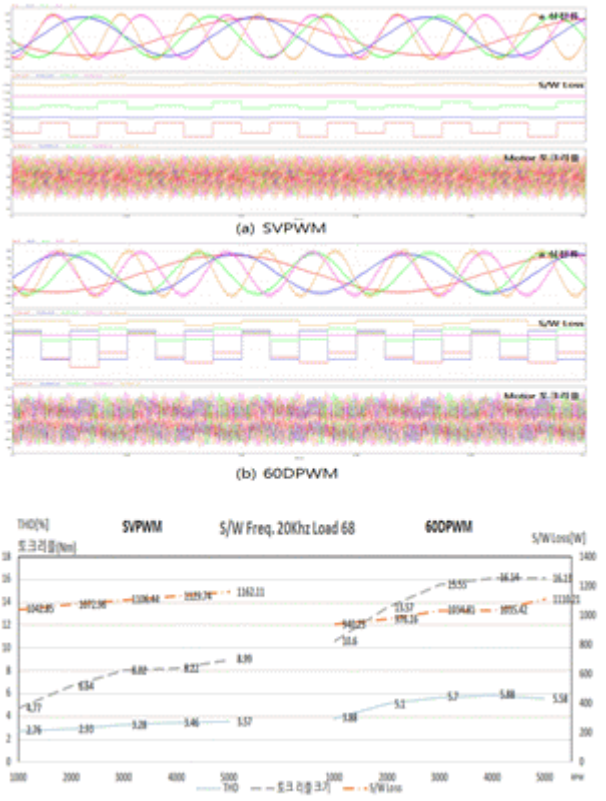

Fig. 10 Switching frequency 20 kHz. Ias THD, Motor torque ripple

Table 3 Switching frequency 20 kHz. Ias THD, S/W Loss, Motor torque ripple

20 kHz	SVPWM			60DPWM		
	THD [%]	S/W Loss [W]	Torque ripple [Nm]	THD [%]	S/W Loss [W]	Torque ripple [Nm]
1000 [RPM]	2.76	1042.85	4.77	3.88	940.25	10.6
2000	2.93	1072.96	6.64	5.1	976.16	13.57
3000	3.28	1106.44	8.02	5.7	1034.81	15.55
4000	3.46	1129.74	8.22	5.88	1035.42	16.14
5000	3.57	1162.11	8.99	5.58	1110.21	16.13

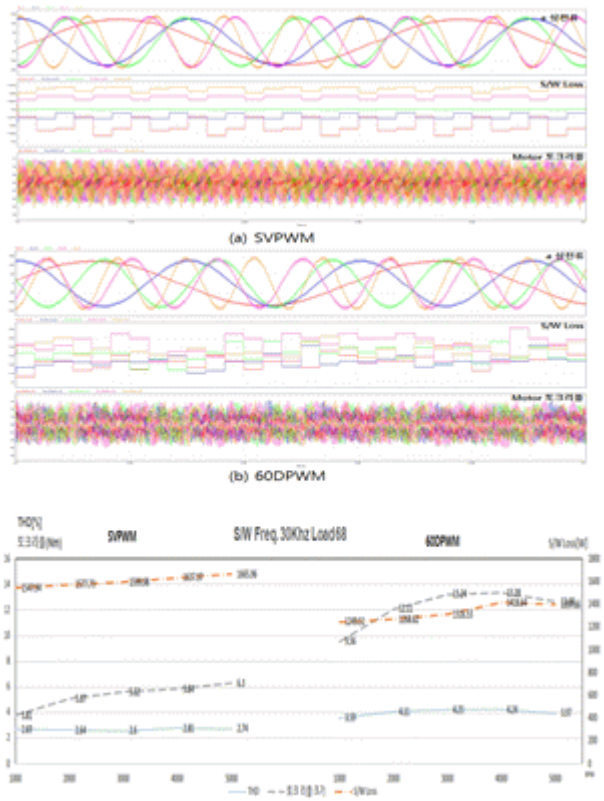

Fig. 11 Switching frequency 30 kHz. Ias THD, Motor torque ripple

Table 4 Switching frequency 30 kHz. Ias THD, S/W Loss, Motor torque ripple

30 kHz	SVPWM			60DPWM		
	THD [%]	S/W Loss [W]	Torque ripple [Nm]	THD [%]	S/W Loss [W]	Torque ripple [Nm]
1000 [RPM]	2.69	1547.94	3.81	3.59	1249.51	9.56
2000	2.64	1577.73	5.07	4.11	1268.62	12.11
3000	2.6	1599.98	5.62	4.23	1316.53	13.24
4000	2.81	1637.97	5.84	4.24	1418.64	13.39
5000	2.74	1665.96	6.3	3.97	1397.66	12.68

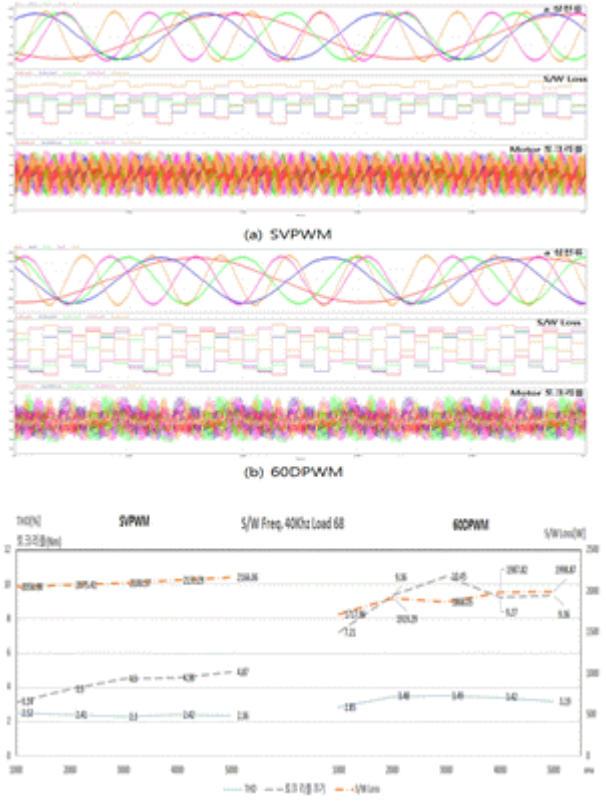

Fig. 12 Switching frequency 40 kHz. Ias THD, Motor torque ripple

Table 5 Switching frequency 40 kHz. Ias THD, Motor torque ripple

40 kHz	SVPWM			60DPWM		
	THD [%]	S/W Loss [W]	Torque ripple [Nm]	THD [%]	S/W Loss [W]	Torque ripple [Nm]
1000 [RPM]	2.52	2056.98	3.14	2.85	1717.96	7.21
2000	2.41	2075.41	3.9	3.48	1919.29	9.36
3000	2.3	2100.57	4.5	3.49	1868.05	10.45
4000	2.42	2133.29	4.56	3.42	1987.82	9.27
5000	2.36	2166.06	4.87	3.19	1998.87	9.36

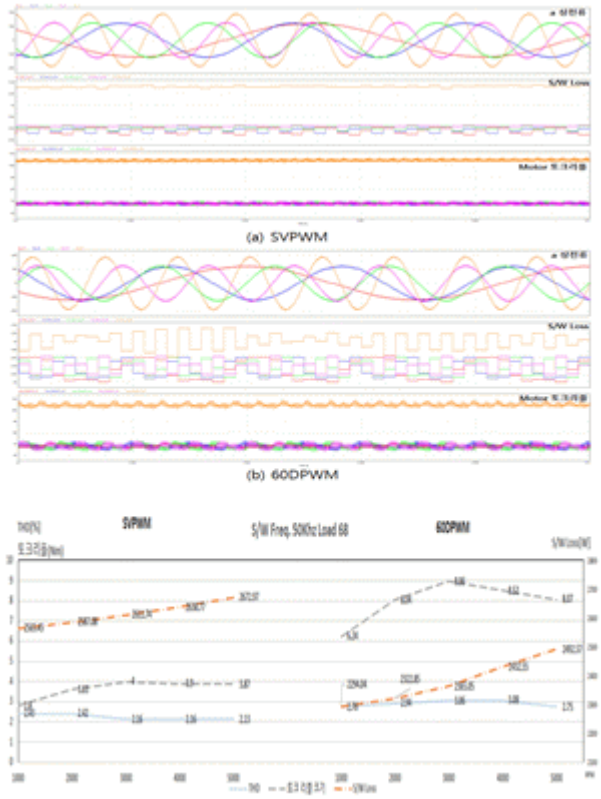

Fig. 13 Switching frequency 50 kHz. Ias THD, Motor torque ripple

Table 6 Switching frequency 50 kHz. Ias THD, Motor torque ripple

50 kHz	SVPWM			60DPWM		
	THD [%]	S/W Loss [W]	Torque ripple [Nm]	THD [%]	S/W Loss [W]	Torque ripple [Nm]
1000 [RPM]	2.43	2565.45	2.8	2.76	2294.04	6.24
2000	2.42	2587.08	3.63	2.94	2322.85	8.04
3000	2.16	2611.74	4	3.06	2365.05	8.96
4000	2.16	2638.77	3.9	3.08	2432.55	8.52
5000	2.13	2672.97	3.87	2.75	2492.57	8.07

The simulation results are summarized in Tables 7 to 9. The results are presented as values of (SVPWM − 60DPWM). Results with negative values indicate that the 60DPWM value is greater and results with positive values indicate that the SVPWM value is greater. According the results of the tests, one can see that SVPWM method exhibits superior performance compared to the 60DPWM method in terms of THD and motor torque ripple, whereas the 60DPWM method exhibits superior performance in terms of switching loss. The THD and motor torque ripple exhibit large differences at low switching frequencies, but these difference are reduced at high switching frequencies. In contrast, in terms of switching loss, the value of the 60DPWM method decreases as the switching frequency increases. Based on the nature of aircraft, which require the use of a motor with high specific power, control performance is poor if a low switching frequency is adopted, so a high switching frequency must be adopted. Therefore, to achieve high-efficiency control of the inverter, it is expected that reliable system operation can be achieved through the variable use of SVPWM and 60DPWM methods depending on the target scenario.

Table 7 Comparison of SVPWM and 60DPWM phase current THDs according to switching frequency

THD [%]	10 kHz	20 kHz	30 kHz	40 kHz	50 kHz
1000 rpm	−2.68	−1.12	−0.90	−0.33	−0.33
2000 rpm	−3.96	−2.17	−1.47	−1.07	−0.52
3000 rpm	−4.27	−2.42	−1.63	−1.19	−0.90
4000 rpm	−4.28	−2.42	−1.43	−1.00	−0.92
5000 rpm	-	−2.01	−1.23	−0.83	−0.62

Table 8 Comparison of SVPWM and 60DPWM switching losses according to switching frequency

S/W Loss[W]	10 kHz	20 kHz	30 kHz	40 kHz	50 kHz
1000 rpm	24.41	102.6	298.43	339.02	271.41
2000 rpm	22.59	96.8	309.11	15.12	264.23
3000 rpm	38.97	71.63	283.45	232.52	246.69
4000 rpm	−0.98	94.32	219.33	145.47	206.22
5000 rpm	-	51.9	268.3	167.19	180.4

Table 9 Comparison of SVPWM and 60DPWM motor ripples according to switching frequency

Ripple [Nm]	10 kHz	20 kHz	30 kHz	40 kHz	50 kHz
1000 rpm	−8.35	−5.83	−5.75	−4.07	−3.44
2000 rpm	−10.12	−6.93	−7.04	−5.46	−4.41
3000 rpm	−12.66	−7.53	−7.62	−5.95	−4.96
4000 rpm	−12.85	−7.92	−7.55	−4.71	−4.62
5000 rpm	-	−7.14	−6.38	−4.49	−4.20

5. Conclusion

In this study, phase current THD, switching loss, and motor ripple were analyzed through simulations to compare PWM methods. In the case of a motor with high specific power for use in an aircraft, a high switching frequency should be adopted to achieve reliable control performance and reduce noise and vibration. When using a switching frequency of 30 kHz or more, the switching loss with the DPWM method is 13.98% less than that with the SVPWM method on average. However, the DPWM method is expected to yield greater noise and vibration than the SVPWM method as a result of greater values of THD and torque ripple. According to the results of this study, it is expected that under the current operating conditions of eVTOL aircraft, if the operating conditions of the inverter are accurately determined within the allowable range of switching loss and noise, and can be varied according to the target scenario, more reliable and efficient system operation can be achieved.

Acknowledgments

This research has been conducted as part of the “Multiple Electric Propulsion Core System Technology Research” project supported by the National Research Council of Science and Technology (Main project of the Korea Aerospace Research Institute).

References

[1] I. H. Choi, B. S. Koo, and S. H. Cho, “Research on PWM Modulation Characteristics of eVTOL thrust motor controlling Inverter” *KSAS2019 Fall Conference*.

[2] S. H. Cho, S. H. Kim, B. S. Koo, I. H. Choi, H. S. Jun, and J. M. Kim, “Selection of Optimal Switching Frequency according to Battery Capacity of 2-level inverter for Driving Electric Propulsion Aircraft”

[3] Bon. Soo. Koo, Seong. Hyeun. Cho, and In. Ho. Choi, “Analysis of Inverter Losses according to Switching Frequency Using Electric Motor for Aircraft,” *Journal of Aerospace System Engineering*, vol. 1, no. 15, 2021.

[4] H. W. Van Der Broeck, H. C. Skudelny, and G. V. Stanke, “Analysis and Realization of a Pulse Width Modulator Based on Voltage Space Vectors,” *IEEE Trans. on Industry Applications*, vol. 24, no. 1, pp. 142–150, 1988.

[5] P. Thamizhazhagan and S. Sutha, “Analysis of PWM Techniques ofr Power Quality Improvement in PMSM Drives,” *Indian J. of Science and Technology*, vol. 8, no. 24, pp. 1–5, 2015.

[6] B. G. Lee, “High Efficiency DPWM Method of 3-Level Inverter using the Offshore Wind Farm,” Sungkyunk Wan University (SKKU), pp. 124, Feb. 2015.

[7] Manual for EMRAX Motors/Generators, Version 5.4, March 2020.

[8] SEMIKRON SKiiP 26GB12T4V1, Data sheet Rev 2.0 Nov. 2017.

[9] S. T. Lee, “A Study on the High Efficiency Operation of Inverter for PMSM Using Transition Control Technique between Driving Methods,” Kongju National University, pp. 198, Feb. 2020.

[10] C. H. Sridevi, I. Ravikiran, “Comparative Analysis of SVPWM and DSVPWM Control Techniques for a Single-Phase to Three-Phase Conversion System,” *IJSR*, vol. 4, pp. 2506–2512, July 2015.

[11] J. Y. Yoo, “Study on PWM for reduction of common-mode voltage and torque ripple in inverter-fed-motor drives,” Korea University, pp. 145, Feb. 2020.